Communications on Applied Nonlinear Analysis
ISSN: 1074-133X
Vol 31 No. 8s (2024)

Routing through LEO Satellite Constellation Networks: A DopplerShift Measurement based Coverage window Detection Approach

Eman Adel Elbehiry[1],[2]*, Ahmed Fares[4],[1]†, Basem M. Elhalawany[1],[5]†, Heba A. Tag.ElDien[1].[3]†

[1]*Electrical Engineering Department, Faculty of Engineering, Shoubra,Benha university, Cairo, 11672, Cairo, Egypt.

[2]Communication Engineering Department, Giza Higher Institute for Engineering and Technology, Giza, Egypt.

[3]Communication Systems Engineering Department, Benha National University, , ElObour, 11828, Cairo, Egypt.

[4]Faculty of Engineering, School of Electronics, Communications and Computer Engineering (ECCE), The Egypt-Japan University for Science and Technology(E.JUST), New Borg Al-Arab, 21934, Alexandria, Egypt.

[5]Electronics and Communication Engineering Department , Kuwait College of Science and Technology, Doha District, Block 4, 93004, Kuwait

*Corresponding author(s). E-mail(s): Eman.Adel@GEI.edu.eg; Contributing authors: ahmed.fares@ejust.edu.eg; basem.mamdoh@feng.bu.edu.eg; Hebaallah.shatat@feng.edu.eg; Hebaallah.shahat@eng.bnu.edu.eg

†These authors contributed equally to this work.

Article History:

Received: *15-05-2024*

Revised: *27-06-2024*

Accepted: *14-07-2024*

Abstract:

Most Internet-of-Things (IoT) applications via satellite depend on reasonably priced, energy-constrained, location-aware IoT sensors. In this letter, we present a brand technique that uses straightforward Doppler measurements to estimate the satellite visibility window on Internet of Things devices. We provide two cases where the IoT device does not initially know the geographic coordinates of the serving satellite: (i) we assume that the IoT device knows the coordinates, and (ii) we assume that the coordinates are unknown. As a result, we obtain the Doppler measurement likelihood function and reduce it to a problem of minimizing root mean square error (RMSE). We use a stochastic optimizer to minimize the root mean square error (RMSE) to predict the orbital parameters of the serving satellite from a series of Doppler observations. We then forecast the satellite visibility window (satellite pass) based on the orbital estimation. We compute the overlapping visibility window between the ground truth and the estimation using the intersection-over-union metric in order to assess the correctness of the window estimation. The results are based on extensive MATLAB simulations. In addition to the proposed technique utilizing Doppler measurements for estimating satellite visibility windows in IoT devices, the system is structured around two ground stations. These ground stations are interconnected through a process facilitated by Dijkstra's Algorithm, which calculates the shortest path between them via visible satellites. This integration of Dijkstra's Algorithm ensures optimal routing and connectivity between the ground stations, enhancing the efficiency and reliability of the IoT application over satellite communication.

Keywords: IoT via satellite, LEO Satellite Constellation, DopplerShift Measurement, Dijkstra Routing Algorithms, Orbit Determination.

1. Introduction

The rapid expansion of Internet-of-Things (IoT) applications via satellite is primarily fueled by the affordability and accessibility of satellite platforms, particularly those in w Earth orbit (LEO) [1, 2]. LEO satellites are favored due to their lower development and deployment costs, despite the challenge of their short visibility windows caused by high relative speeds. Many IoT solutions rely on simple

protocols that transmit brief, sporadic messages. Therefore, aligning these transmissions with the satellite's visibility window is crucial to enhance transmission success rates and prolong IoT device lifespans. Accurate alignment between the satellite and the ground device is vital not only for reliable data transmission but also for determining the ground device's position [3]. To effectively schedule IoT transmissions, it is necessary to estimate the satellite's visibility window, which requires understanding the satellite's orbit. This estimation can be done using two main types of observations: radio measurements (such as radar, Doppler observations, radio ranging, and interferometry) and optical observations (such as visual, photographic, and laser ranging measures) [4]. Six key elements define an orbit in Keplerian motion: the semi-major axis, eccentricity, inclination angle, argument of periapsis, true anomaly, and the right ascension of the ascending node. Traditional methods for orbit determination include the Gaussian, Gibbs, and

Laplacian methods [4].The Gaussian method calculates velocity using the observation interval and two orbital points but has limited applications due to the small allowable spread between true anomaly angles [5]. The Gibbs method provides a more accurate estimate using three position observations, independent of time unless necessary to determine the satellite's position on the ellipse. The Laplacian method fully defines the orbit using three observations of time, declination, and right ascension [6]. While these traditional methods have been effective for tracking celestial bodies, they are less suitable for IoT applications where basic IoT sensors cannot calculate positions or angles. Modern methods have evolved to overcome these limitations. The least-squares (LS) technique fits a computed curve to Doppler measurements, iteratively refining the six Keplerian orbital parameters until they converge to the true orbit [7]. Another approach uses the SGP4 model and NORAD two-line element (TLE) information or a perturbed circular motion prediction model to estimate orbits from telemetry radio measurements without relying on the NORAD database [8]. The maximum likelihood estimation (MLE) technique generates optimal parameter estimates by maximizing the conditional density function of the state based on Doppler observations [9]. These modern methods underscore the importance of Doppler shift measurements in estimating satellite orbits and visibility windows[10, 11] . Effective power conservation in IoT devices can be achieved by activating the transceiver only when the satellite is visible, as determined by these Doppler measurements [12]. This study proposes a framework for deciding satellite visibility windows in two scenarios: (i) when the ground IoT device's geographic location is known via external input, and (ii) when the IoT device is unaware of its location [13, 14]. In the first scenario, even minimal

satellite information, such as height, allows for the estimation of three relative orbital parameters: the orbit's inclination, the right ascension of the ascending node (RAAN), and the initial mean anomaly. In the second scenario, the IoT device must also estimate its latitude in addition to the other three orbital parameters. This comprehensive approach ensures reliable IoT services by effectively aligning transmission schedules with satellite visibility windows. To enhance the IoT communication network, we also need to consider the routing problem for data transmission between ground stations via satellites. On the other hand, the Dijkstra algorithm, a well-known graph search algorithm that finds the shortest path between nodes, can be employed to determine the best path for data transmission[15]. By representing the ground stations and satellites as nodes

and the communication links as edges with associated weights (such as transmission delay or signal loss), we can apply the Dijkstra algorithm to find the optimal path between Ground Station 1 and Ground Station 2 [16]. This involves identifying visible satellites for each ground station and ensuring that the path chosen maximizes the visibility window and minimizes transmission interruptions. By incorporating the Dijkstra algorithm into the scheduling framework, we can further optimize IoT data transmissions, ensuring efficient and reliable communication through LEO satellites[17, 18].

Motivation and Contributions

This work exploits the Doppler shift measurement approach introduced in [19] for the visibility window detection for all satellites covering both ground stations. The work in [19] explored different optimization techniques for estimating the satellites orbital parameters, including obtaining the Doppler measurement likelihood function and reducing it to a problem of minimizing the root mean square error (RMSE). The authors in [19], have used a stochastic optimizer to minimize the root mean square error (RMSE) and estimate the orbital parameters of the serving satellite from a series of Doppler observations where PSO achieved the best results. In this work, we have proposed ACO optimization as an alternative that outperforms PSO and other techniques.

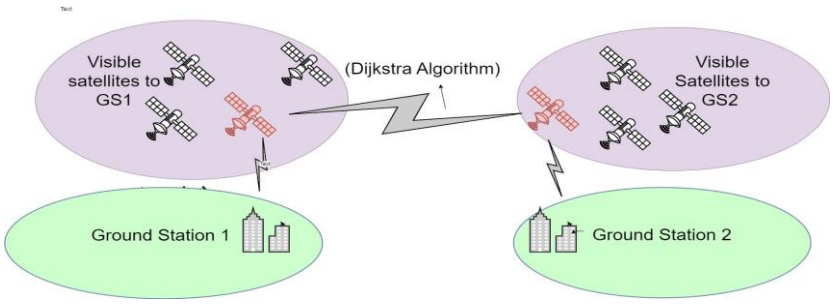

Fig. 1 Description of the system

Description of System

This study aims to implement a novel methodology tailored for eMTC applications within IoT networks. The proposed system integrates geometric representations of ground stations' observable satellites and applies Dijkstra's routing algorithms to establish efficient communication paths. Additionally, a Doppler measurement error model is employed to estimate the visibility window of satellites, enhancing the accuracy and reliability of satellite-ground station communication links. The methodology is structured around four primary components:

Geometric Representation and Dijkstra Routing Algorithms:

We create a detailed geometric representation of the satellites observable from each ground station. This involves mapping the spatial positions and trajectories of the satellites relative to the ground stations. Using this geometric framework, we apply Dijkstra's routing algorithm to determine the most efficient communication paths, as shown in fig 1. Dijkstra's algorithm is a well-known graph search algorithm that finds the shortest path between nodes in a graph, which may represent, for example, road networks, routing of data, or, in our case, satellite communication links. The algorithm works by iteratively selecting the node with the smallest known distance from the source and updating the path

lengths of its neighbouring nodes. The steps of the Dijkstra algorithm are summarized in Algorithm 1. Finally, the block diagram in Figure 2 shows the overall system.

Steps of routing from ground station 1 to ground station 2

Calculate the satellites' elevation angles about the ground stations Thus, use advance to represent the initial time step scenario. Next, ascertain each satellite's elevation angle concerning the ground stations using an aerometer. Assume that the minimum threshold elevation angle needed to achieve communication between satel- lites and both ground stations is 30 degrees[20]. Find the elevation angles that are larger than or equal to this value as a result.

Choose the Best Satellite for Constellation's First Access It is believed that the satellite that simultaneously fits the following criteria will be the best choice for initial access to the big constellation:

-The range that is closest to the "Target Ground Station" and possesses an elevation angle from the "Source Ground Station" of at least 30 degrees.

The logic used to identify the first satellite is also applied to find the remaining nodes in the path. "Target Ground Station" is the next node along the path, if the elevation angle of the satellite at the current node is already at least 30 degrees about it. If not, similar reasoning to that used to identify the first satellite in the path is applied to select the next node in the constellation.

-The range that is closest to "Target Ground Station"

-The present node's elevation angle concerning the satellite is more than or equal to -15 degrees.

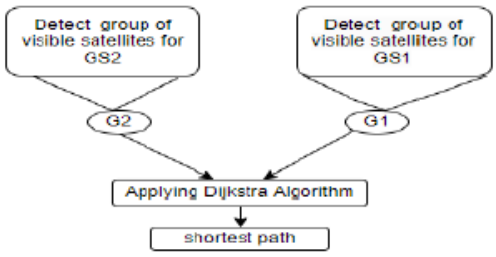

Fig. 2 Block Diagram of Dijkstra's Algorithm in Satellite Routing

Algorithm 1 Dijkstra Algorithm for shortest-path Between Ground Stations via Visible Satellites

Input: Graph $G(V, E)$ with vertices V and edges E, source ground station s, destination ground station t
Output: Shortest path from s to t

Initialize distance $dist[v] \leftarrow \infty$ for all vertices $v \in V$
$dist[s] \leftarrow 0$
Initialize priority queue $Q \leftarrow \{s\}$
Initialize predecessor array $pred[v] \leftarrow$ null for all vertices $v \in V$
while $Q \neq \emptyset$ **do**
    $u \leftarrow \text{ExtractMin}(Q)$
    for each neighbor v of u **do**
        if $dist[u] + \text{weight}(u, v) < dist[v]$ **then**
            $dist[v] \leftarrow dist[u] + \text{weight}(u, v)$
            $pred[v] \leftarrow u$
            $Q \leftarrow Q \cup \{v\}$
        end if
    end for
end while

Path Construction:
Initialize path array $path \leftarrow []$
$current \leftarrow t$
while $current \neq$ null **do**
    Insert $current$ at the beginning of $path$
    $current \leftarrow pred[current]$
end while

Return $path$

The horizon is approximately -21.9813 degrees about each satellite in the constella- tion, which is why the elevation value of -15 degrees was selected. Assuming a spherical Earth geometry and that these satellites are positioned at an approximate altitude of 500 kilometers in near-circular orbits, this value can be obtained. Be aware that the elevation angle of the horizon below is the only calculation that uses the spheri- cal Earth assumption. The angle of horizon elevation = -21.9813 It is assumed that a satellite will be visible to another satellite if its elevation angle relative to it is larger than -21.9813 degrees. Still, -15 degrees gives you a good margin of safety. Until the path reaches a satellite whose elevation angle concerning the ”Target Ground Station” is at least 30 degrees, the next nodes are added one after the other. The routing is finished, and the ”Target Ground Station” is the last node.

Satellite Orbit Geometric Model

Six fundamental parameters can be used to describe a Keplerian orbit fully:

1. Semi-major axis a;
2. Eccentricity e, which defines the oblateness of the orbit;
3. Inclination angle i, which is the angle between the equatorial plane and orbital plane;
4. Right ascension of the ascending node **Ω**, which is the orbital plane’s rotation from the reference axis;
5. Argument of periapsis ω, which is the angle from the ascending node to the perigee point; however, in a circular orbit scenario, there is no perigee point, so this angle can be set to zero without losing generality;
6. True anomaly, which is the angle between the perigee point and the satellite’s position at a specific reference time.

A circular orbit with three orbital parameters—RAAN **Ω**, initial mean anomaly θ, and inclination i—is shown in Fig 3. Without sacrificing generality, we concentrate in this letter on polar-orbiting low-

Earth orbit (LEO) satellites, such as OneWeb, Starlink, authorized licensed, and Iridium, where the orbital inclination can be in the range of i ∈ [60◦, 90◦] and the altitude h ∈ [200 km, 2000 km].

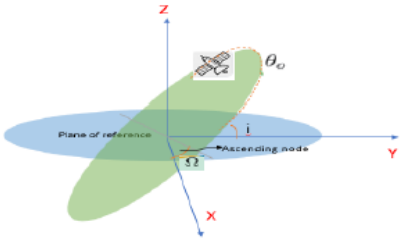

Fig. 3 A representation of an orbiting satellite element in circular orbit

Doppler Measurement Model:

The Doppler effect plays a significant role in satellite communication, influencing the accuracy of signal transmission and reception. To account for this, we develop a Doppler measurement error model that estimates the satellite's visibility window. This model helps in predicting the periods during which a satellite is within optimal range and alignment for communication with a ground station. By incorporating Doppler shift calculations, we can enhance the precision of timing and frequency adjustments, leading to more reliable data transfer. Tables I and II provide a comprehensive list of pertinent symbols and notations used in the description of ground stations 1 and 2, respectively. These tables, along with the geometric representations and routing algorithms, form the core of our proposed system. Figure 1 illustrates the overall system architecture and the interactions between its components. The remainder of this document is structured as follows: Section II delves into the geometric representation and Dijkstra's algorithm application, outlining the methodologies and algorithms used. Section III details the Doppler measurement error model

and its implementation. Section IV presents the experimental setup, results, and discussions,

highlighting the effectiveness of our proposed system in real-world scenarios. Finally, Section V concludes the study with a summary of the findings and potential future research directions.

Finally, the combination of geometric representation, Doppler measurement error modeling, and Dijkstra's routing algorithms provide a strong foundation for improving eMTC applications in extensive IoT installations. This methodology opens the door for future developments in IoT network design and optimization in addition to increasing the effectiveness and dependability of satellite-ground station communications. Due to their lower power budget, low-Earth orbit (LEO) satellites are also better suited for Internet of Things applications. As a result, we use the provided Keplerian orbital elements in conjunction with the Simplified General Perturbations 4 (SGP4) propagator to generate the ground truth orbit. The secular and periodic fluctuations brought about by Earth's geometry and atmospheric drag are taken into consideration by SGP4. The propagator works well with satellites that have fewer than 225 minutes in orbit

Table 1 NOTATIONS AND SYMBOLS

Symbol	Definition	value [Unit]
α	Orbit's semi-major axis	7571[Km]
e	Orbit's eccentricity	0
h	Satellite's altitude	1200 [Km]
T	Orbital period	109.26 [min]
μ_G	Geocentric gravitational constant	$3.986 \times 10^{14}\ m^3/s^2$
Ω	Right ascension of ascending node	240°
θ	Initial mean anomaly	−60°
v	Relative velocity	−[m/s]
ρ	Slant Distance between satellite and ground device	-[m]
t	Time variable	−[s]
Δt	Sampling time	15[s]
f_d	Doppler shift frequency measurement	−[Hz]
μ_d	True Doppler shift frequency	−[Hz]
σ_d	Standard deviation of Doppler shift measurement	[10 Hz]
Θ	Latitude of IoT ground device	−23.5°
ϕ	Longitude of IoT ground device	136°

Table 2 NOTATIONS AND SYMBOLS

Symbol	Definition	value [Unit]
α	Orbit's semi-major axis	7571[Km]
e	Orbit's eccentricity	0
h	Satellite's altitude	1000 [Km]
T	Orbital period	109.26 [min]
μ_G	Geocentric gravitational constant	$3.986 \times 10^{14}\ m^3/s^2$
Ω	Right ascension of ascending node	240°
θ	Initial mean anomaly	−60°
v	Relative velocity	−[m/s]
ρ	Slant Distance between satellite and ground device	-[m]
t	Time variable	−[s]
Δt	Sampling time	15[s]
f_d	Doppler shift frequency measurement	−[Hz]
μ_d	True Doppler shift frequency	−[Hz]
σ_d	Standard deviation of Doppler shift measurement	[10 Hz]
Θ	Latitude of IoT ground device	42.3001°
ϕ	Longitude of IoT ground device	−71.3504°

Doppler Measurement equations

The change in frequency of the signal induced by the relative velocity of the transmitter (a satellite) and the receiver (an Internet of Things device) is known as the Doppler shift. The model presupposes that the ground IoT device receiver is stationary concerning the Earth-centered Earth-fixed coordinates (ECEF) and that the satellite transmitter is in a specific orbit around the Earth. One way to calculate the relative radial velocity is as follows:

$$v(t) = \lim_{\Delta t \to 0} \frac{\rho(t + \Delta t) - \rho(t)}{\Delta t} \qquad (1)$$

where Δt is the simulation time step, t is the time variable, and ρ is the slant distance between the satellite and the ground device. The measurements pass the normality test with 97.8% confidence, showing that the Doppler error distribution bears a reasonable resemblance to the normal distribution. As a result, the Doppler shift measurement is expressed as $f_d \sim (\mu_d, \sigma^2)$, where σ_d is the standard deviation and μ_d is the true Doppler shift, which is determined by $\mu_d = cv/f_c$, where f_c is the carrier frequency and c is the speed at which light propagates in vacuum.

Satellite Visibility Window Analysis Instructions

The timing, the observer's position, and the satellite's orbit all affect the visibility window and satellite

passes. As a result, the satellite orbit is propagated and iteratively sampled using a fine temporal grid to compute the visibility prediction [21]. But this is only going to be feasible if we already know the satellite's orbit. Utilizing the easily accessible Doppler measurements as an inverse problem, our goal is to estimate the orbit and, consequently, future visibility windows.

Visibility Window

The measurement of a satellite's elevation angle (ν) with regard to an observer is made between the observer's local horizon and the satellite point. Based on the locations of the observer and satellite, the angle can be computed. Thus, the satellite is considered visible when its elevation angle ζ is greater than a minimal threshold ζh. The visibility window(s) at a given time interval [a, b] can therefore be written as follows:

$$W = \{t \in [a, b] : \zeta > \zeta_h\} \quad (2)$$

We use a double transmitting satellite and two ground IoT devices in the experiment. First, as described in the next section, we propagate the orbital scenario and derive Doppler measurements from the simulated geometry for two ground Stations with visible satellites for each ground Station. As a result, we estimate the orbit using the first two passes, and we check the accuracy of the estimation using the subsequent passes. The results that were achieved are based on all measurements, and the following is an additional explanation of the simulation steps.

Orbit Determination

Using the Doppler shift frequency observations, we first estimate the satellite's orbit in this manner. In addition to the observer position, all six of the previously listed parameters must be determined to adequately describe an orbit. We lower the number of orbital parameters that must be estimated to simplify the computation. Among IoT applications, we look into the following two scenarios:

Case 1: The inclination, RAAN, and initial mean anomaly are the three orbital characteristics

of the satellite that we estimate. This is so that we may assume e = 0 and the argument of periapsis at zero without losing generality since we are assuming a typical example of a circular orbit. We also assume that we know the height. Furthermore, it is believed that the IoT ground device's location is known.

Case 2: We estimate the latitude of the ground-based IoT device in addition to the parameters from Case 1. Keep in mind that since the orbit is based on the device's timing and assumes its longitude to be the meridian, we do not need to know the longitude of the device. The satellite's altitude is the sole known parameter.

Likelihood Function

Given a set of orbital parameters and location, we calculate the probability function that represents the Doppler observations to predict the orbital parameters. Then, we use a stochastic optimizer to discover the parameters such that we can maximize the function. Consequently, in example 1 and case 2, respectively, the state vector is x = [i,Ω, θo, Θ] , where Θ is the IoT device's latitude. Given

the normal distribution of Doppler shift measurements, the probability function may be written as follows:

$$p(f_d^{(k)}|x) = \frac{1}{\sqrt{2\pi}\cdot\sigma_d}\cdot\exp\left(-0.5\cdot\left(\frac{f_d-\mu_d}{\sigma_d}\right)^2\right) \quad (3)$$

where f_d is the measured Doppler shift frequency at time index k, μ_d is the true Doppler shift frequency which depends on the state vector x, and σd is the error standard deviation. We can simplify the likelihood maximization problem, based on K measurements, into a root mean squared error (RMSE) minimization problem, as follows,

$$\begin{aligned} -\ln p(f_d^{(k)}|x) &= -\ln C\left(\prod_{k=1}^{K}\exp\left(-\frac{(f_d^{(k)}-\mu_d^{(k)}(x))^2}{2\sigma_d^2}\right)\right) \\ &= \sum_{k=1}^{K}\left(-\frac{(f_d^{(k)}-\mu_d^{(k)}(x))^2}{2\sigma_d^2}\right)+C \\ \epsilon(x) &= \sqrt{\sum_{k=1}^{K}\frac{1}{K}\left(f_d^{(k)}-\mu_d^{(k)}(x)\right)^2} \end{aligned} \quad (4)$$

which represents the RMSE between the measured Doppler vector and the calculated mean based on the orbital geometry. $C = 1\sigma_d\sqrt{2\pi}$ is a constant, which does not contribute to the issue of depreciation. We use a stochastic optimizer to minimize the RMSE, which is the same as maximizing the likelihood function. An effective optimization technique called Ant Colony Optimization (ACO) was developed in response to the way ants use pheromone trails to determine the shortest route between their nest and food sources [22]. Compared to Particle Swarm Optimization (PSO), ACO has a number of advantages when it comes to reducing Root Mean Square Error (RMSE). ACO's strong exploration capacity is one of its main advantages since it enables it to thoroughly examine intricate, multi-modal environments without prematurely converging to local minima. ACO's pheromone system continuously modifies itself in response to the caliber of solutions discovered, guaranteeing ongoing adaptation and advancement. As a result, ACO performs particularly effectively in scenarios with a large number of local optima and a complex search space. Moreover, ACO's ability to balance exploitation and exploration through pheromone evaporation and deposition ensures a more exhaustive search process. PSO is known for its ease of use and quicker convergence; nonetheless, it sometimes runs the danger of converging too soon to sub-optimal solutions, especially in complex environments [23]. For optimization tasks requiring through exploration and robust global search, like minimizing RMSE in challenging circumstances, ACO is hence a preferable choice over PSO.

Discussion and Results

In this study, a single transmitting satellite and a receiving IoT device were used to propagate an orbital scenario and derive Doppler measurements, with key observations including elevation angle and Doppler shift patterns relative to the visibility window. The shortest path between two ground stations was determined using Dijkstra's algorithm, selecting satellites based on elevation angles to ensure optimal communication. Various stochastic optimization strategies were tested to minimize RMSE, with the particle swarm optimizer performing best. The Ant Colony Optimization algorithm,

which balances exploration and exploitation, was highlighted for its efficiency. Lastly, the visibility window estimation was evaluated using the intersection-over-union measure, indicating the accuracy of the estimated parameters.

Visibility Window with Elevation Angle and Doppler Shift

We use a single transmitting satellite and a receiving Internet of Things device on the ground in the experiment. First, we propagate the orbital scenario and derive Doppler measurements from the simulated geometry. Figure 4 illustrates the relationship between the elevation angle, Doppler shift, and the visibility window of the satellite. Key observations include: The elevation angle peaks when the satellite is directly overhead, providing the maximum signal strength. The Doppler shift exhibits

a characteristic curve, starting from a positive value, decreasing through zero (when the satellite is overhead), and becoming negative as the satellite moves away. The visibility window, estimated based on elevation angle thresholds, aligns well with the periods of significant Doppler shifts. As a result, we estimate the orbit using the first two passes and check the accuracy of the estimation using the subsequent passes. Fig. 4 shows the elevation angle and Doppler shift with the visibility window.

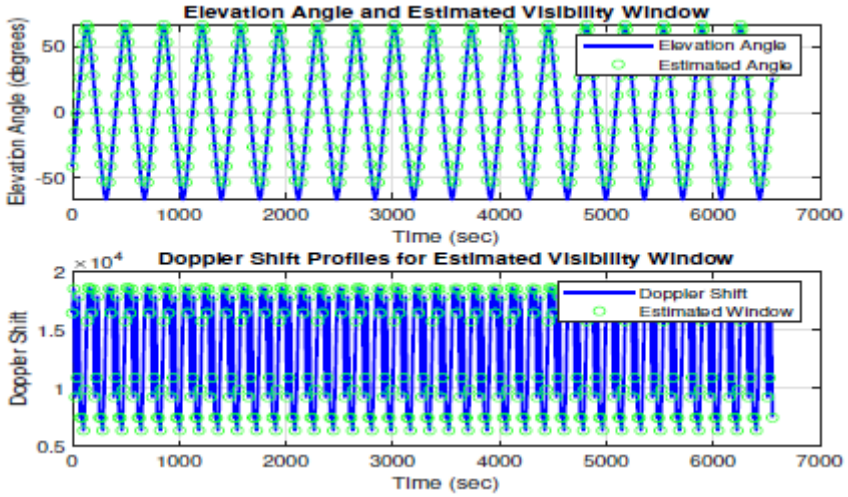

Fig. 4 Visibility Window with Doppler shift and Elevation angle

Ground Stations with Visible Satellites

Figure 5 shows the positions of the two ground stations and their respective visible satellites. Important points include: Each ground station is linked to multiple satellites that are within its line of sight. The visibility of satellites varies over time due to the orbital motion, as indicated by the dynamic links between ground stations and satellites. Fig 5 shows the two ground stations with visible satellites for each ground station. The shortest path between the visible satellites linked to Ground Station 1 and

the visible satellites linked to Ground Station 2 is determined using Dijkstra's algorithm. This ensures the most efficient route is selected for data transmission between the two ground stations, optimizing communication performance.

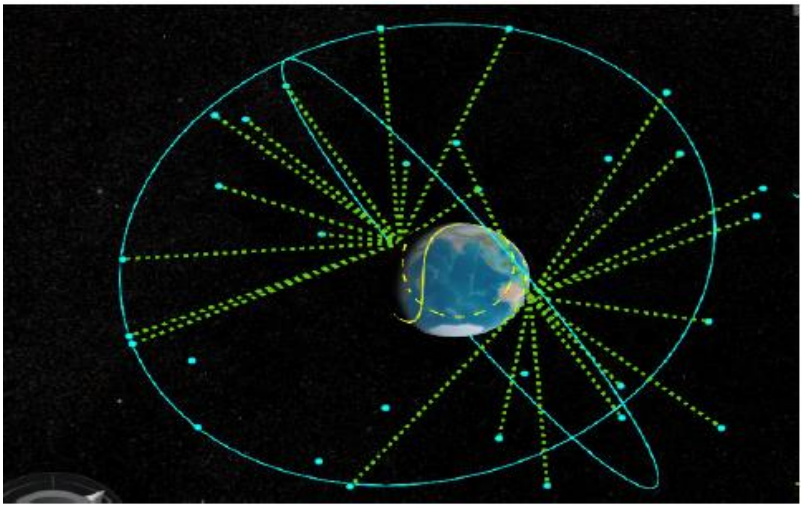

Fig. 5 Every ground station linked to every satellite in view for its

Route using Dijkstra Algorithm

The main topic of this study is the application of satellite constellations for routing from Ground Station 1 to Ground Station 2. The elevation angles of the satellites concerning the ground stations at the start time are calculated as part of the routing process. To guarantee a minimum 30-degree elevation difference, satellites are chosen according to their elevation angles for the source and target ground stations, as shown in figure 6. The satellite most suited for first access to the constellation depends on how close it is to the intended ground station and how high it is above the source ground station. Similar selection criteria are used for subsequent nodes along the path to the target ground station, ensuring that each node maintains an appropriate elevation angle for communication. the shortest path using the Dijkstra Algorithm with the determination of the source ground station and the target ground station is shown in figure 7.

Stochastic Optimizer

Pattern search (PS), simulated annealing (SA), genetic algorithm (GA), multi-objective genetic algorithm (MOGA), particle swarm (PSO), Ant Colony Optimization (ACO), and surrogate optimization (SO) are a few of the stochastic optimization strategies available. To identify the best optimizer for this particular situation, we thus examine the performance using a variety of optimizers. As a result, we execute the optimizers and the identical satellite orbit. The optimizer seeks to minimize the RMSE cost function in by identifying the best state vector.

$$x = \text{argmin}_x[\epsilon(x)] \qquad (5)$$

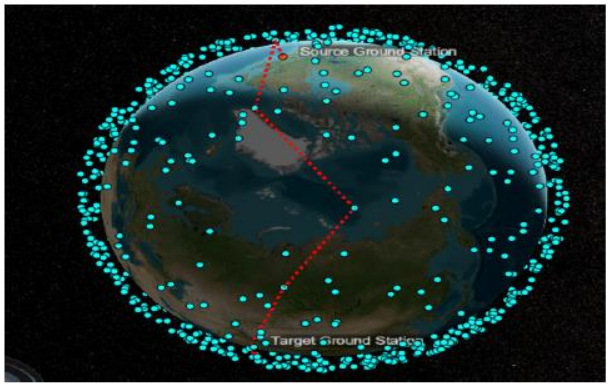

Fig. 6 The path through visible satellites for each ground station.

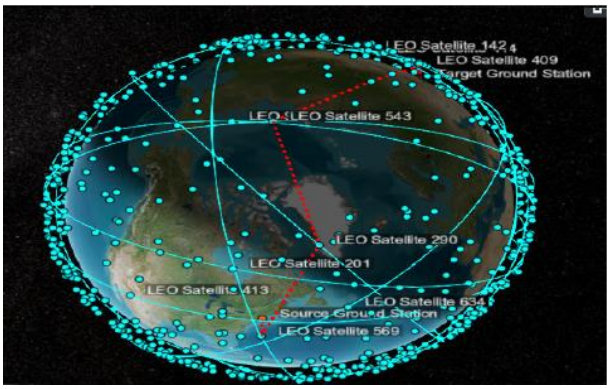

Fig. 7 Shortest path using Dijkstra Algorithm and selection of source ground station and target ground station

where the estimated state vector is denoted by ˆx. Figure 8 shows that the particle swarm optimizer performs the best in terms of minimizing the objective function. One bio-inspired algorithm called ACO is based on how creatures move in groups, like a flock of birds or a school of fish [24]. Because it includes the diversity and intensification components, it is classified as a metaheuristic optimization method. The organisms in the algorithm, called particles, are dispersed over the solution space, and each particle searches for the best answer or diversification. The intensification part of the procedure is when the particles go toward the good solution region to perform a focused search after they have located a good solution within the space [25].

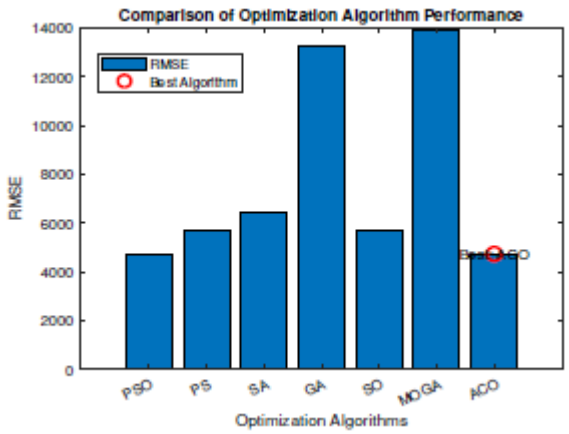

Fig. 8 Comparison between all optimization Algorithms

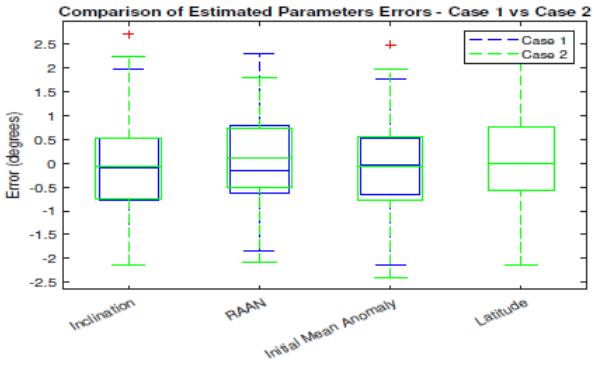

Fig. 9 Boxplot of the estimated parameters errors (inclination, RAAN, initial mean anomaly and latitude) for Case 1 and Case 2.

The algorithm's convergence to the global solution can be ensured by striking a fair balance between these two elements. It is also computationally cheap because it is a straightforward algorithm that just needs elementary mathematical calculations [24].

Results of Orbital Estimation

Fig. 9 displays the statistics of the estimated parameter errors for Case 1 and Case 2. A dot marker is used to show the median error. As can be shown, the error medians of the three orbital parameters for

Case 1 are roughly near to 0◦, and the errors have a tight distribution overall. Case 2 on the other hand, has a larger dispersion and higher error medians than Case 1.

An Assessment of the Visibility Window

We employ the intersection-over-union (IoU) measure, which is frequently used to assess bounding box prediction in machine vision applications, to evaluate the estimation fitness of the visibility window fairly [26]. The satellite visibility window serves as the bounding box in our intersection-over-union (IoU) is calculated by calculating the percentage of overlapping bounding boxes. The computation of the IoU is displayed below.

$$\text{IoU} = \frac{A\cap}{A\cup} = \frac{\hat{W} \cap W}{\hat{W} \cup W} \qquad (6)$$

Measurements with a confidence interval of 97.8%. where A∩ is the area of the intersection, and A∪ is the area of the union of the estimated and the ground truth windows. ˆW represents the estimated visibility window, whereas W denotes the ground truth, which was previously defined in figure 4. We illustrate in figure 10 a further example of the satellite visibility window simulation, showing both the estimated window and the ground truth window. In this example, the true and estimated window are fully overlapping. Figure also shows the estimated and ground-truth Doppler profiles.

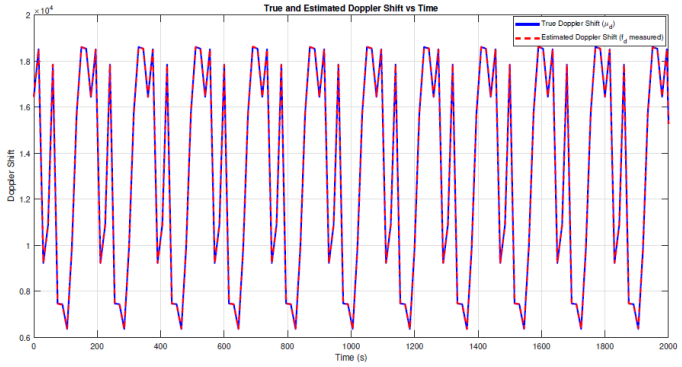

Fig. 10 Comparison between True Doppler Shift and Estimated Doppler Shift

To further evaluate the performance of the proposed framework in estimating the visibility window, we give the IoU statistics comparing two cases: (i) when the measurements from two passes are utilized for the estimation, and (ii) when utilizing the measurements from four passes. The comparison is displayed in , where it is important to highlight that we can increase the prediction's boundaries by using more measurements in the estimation. But in real-world situations, every Doppler measurement has an energy cost. As such, it is a design decision to strike a compromise between the device's battery life and accuracy.

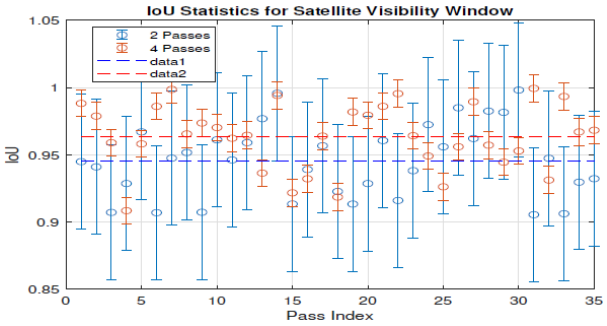

Fig. 11 Statistics of the intersection-over-union (IoU) for satellite visibility window after several passes using two and four passes of Doppler measurements

Future Work

Several exciting new directions for satellite orbit estimation research and development have opened up as we continue to improve our knowledge and methods. Some are enhancing estimating techniques, fusing satellite data with on-the-ground observations, and extending the experimental reach to bigger networks. The precision, dependability, and scalability of satellite communication systems and orbital mechanics research might greatly improve in these fields.

Refinement of Estimation Algorithms

Future work can focus on refining the estimation algorithms to further reduce errors. Machine learning techniques could be explored to enhance the prediction accuracy based on historical data.

Integration with Ground-Based Observations

Combining satellite-derived data with ground-based observations, such as radar or optical tracking, can provide a more comprehensive understanding of satellite orbits and improve estimation accuracy.

Expansion to Larger Networks Scaling

the experiment to include a larger number of ground stations and satellites can provide insights into the scalability and robustness of the proposed methods in more complex networks.

Conclusions

In this correspondence, we introduced a methodology for forecasting the visibility window of a satellite through a sequence of Doppler observations. The satellite's orbit was calculated by obtaining the inclination, RAAN, and starting mean anomaly, which are three orbital factors that determine the probability function of the Doppler measurements. We reduced the probability function maximization to a task of minimizing the root mean square (RMSE). We then used a stochastic optimizer to reduce the root mean square error. We used the intersection-over-union measure to examine the visibility window's accuracy based on the projected orbit. The findings suggest that the Doppler measurements might reasonably approximate the visibility window. In addition, it is imperative to underscore the architectural framework of the system, which comprises two ground stations. Each ground station possesses a distinct set of visible satellites within its field of observation. We leverage the Dijkstra algorithm to optimize

the communication path between these ground stations to establish the most efficient route through the available satellites. This ensures that data transmission between the stations is facilitated along an optimal trajectory, enhancing the overall efficiency and reliability of the system. By integrating this path-finding algorithm into the broader framework, we fortify the operational robustness and performance of the satellite communication network.

List of abbreviations

Ant Colony Algorithm (ACO)

Pattern search (PS)

simulated annealing (SA)

genetic algorithm (GA)

multi-objective genetic algorithm (MOGA)

particle swarm (PSO)

The right ascension of the ascending node (RAAN)

Declatrations

Availability of Data and Materials

The datasets generated and analyzed during the current study are available from the

corresponding author on reasonable request.

Competing Interests

The authors declare that they have no competing interests.

Funding

this research does not have funding from any organization.

Authors' contributions

These authors contributed equally to this work.

Acknowledgements

The authors thank BENHA University for their valuable assistance with [specific aspect of the work, e.g., statistical analysis, data collection]. We also acknowledge the contributions of [Dr Basem Elhalawany ,Dr Heba Adly and Dr Ahmed Fares], whose support and resources were instrumental in completing this research.

References

[1] Marco Centenaro, Cristina E Costa, Fabrizio Granelli, Claudio Sacchi, and Lorenzo Vangelista. A survey on technologies, standards and open challenges in satellite iot. IEEE Communications Surveys & Tutorials, 23(3):1693–1720, 2021.

[2] Fabricio S Prol, R Morales Ferre, Zainab Saleem, Petri V¨alisuo, Christina Pinell, Elena Simona Lohan, Mahmoud Elsanhoury, Mohammed Elmusrati, Saiful Islam, Kaan C, elikbilek, et al. Positioning and timing enhancements for 5g networks via artificial intelligence: a survey. IEEE Communications Surveys & Tutorials, 24(2):1167–1195, 2022.

[3] Kyrillos MP Ebrahim, Sherif MMH Gomaa, Tarek Zayed, and Ghasan Alfalah. Recent phenomenal and investigational subsurface landslide monitoring techniques: A mixed review. Remote Sensing, 16(2):385, 2024.

[4] Yuan Wang, Li Deng, Jingye Yan, Rui Li, Xiucong Sun, Tianshan Dong, and Shenggang Liu. Formation design for interplanetary shock imaging interferometric array. Advances in Space Research, 2024.

[5] Melissa De Iuliis, Marianna Crognale, Francesco Potenza, and Vincenzo Gattulli. On the combined use of satellite and on-site information for monitoring anomalous trends in structures within cultural heritage sites. Journal of Civil Structural Health Monitoring, pages 1–18, 2024.

[6] Zhao Feng, Changxiang Yan, Congjun Wu, and Yanfeng Qiao. Positioning error estimation method for short-arc angles-only initial orbit determination. Journal of Guidance, Control, and Dynamics, pages 1–8, 2024.

[7] Alberto Foss`a, Matteo Losacco, and Roberto Armellin. Perturbed initial orbit determination. Astrodynamics, pages 1–16, 2024.

[8] Lihao Yao, Honglei Qin, Boyun Gu, Guangting Shi, Hai Sha, Mengli Wang, Deyong Xian, Feiqiang Chen, and Zukun Lu. A study on anti-jamming algorithms in low-earth-orbit satellite signal-of-opportunity positioning systems for unmanned aerial vehicles. Drones, 8(4):164, 2024.

[9] Yuanhui Mo, Tao Lai, Qingsong Wang, and Haifeng Huang. A novel methodology for d-gbsar repositioning error compensation based on maximum likelihood estimation. IEEE Transactions on Geoscience and Remote Sensing, 2024.

[10] Xiwei Bai and Li-Ta Hsu. Gnss/visual/imu/map integration via sliding window factor graph optimization for vehicular positioning in urban areas. IEEE Transactions on Intelligent Vehicles, 2024.

[11] Xiaobo Gu, Zeyang Qiu, Yanjiao Wang, and Wei Jiang. Lstm-based clock synchronization
for satellite systems using inter-satellite ranging measurements. GPS Solutions, 28(3):147, 2024.

[12] Mthomasebe Adonis. Design and implementation of internet of things in nanosats. PhD thesis, Cape Peninsula University of Technology, 2024.

[13] Joel Jurado Diaz, Nils Pachler de La Osa, Juan Jose Garau-Luis, Edward F Crawley, and Bruce G Cameron. Satellite routing for mobile users under uncertainty in high throughput constellations. In 2024 IEEE Aerospace Conference, pages 1–13. IEEE, 2024.

[14] Yang Yang, Shengbo Hu, and Guiju Lu. Dynamic caching routing strategy for leo satellite nodes based on gradient boosting regression tree. Journal of Information Processing Systems, 20(1):131–147, 2024.

[15] Ahmed M Khedr, Zaher Al Aghbari, and Pravija PV Raj. Msspp: modified sparrow search algorithm based mobile sink path planning for wsns. Neural Computing and Applications, 35(2):1363–1378, 2023.

[16] Sara Santos, Francisco A Monteiro, Bruno C Coutinho, and Yasser Omar. Shortest path finding in quantum networks with quasi-linear complexity. IEEE Access, 11:7180–7194, 2023.

[17] Vivek AnandMet al. Shortest path optimization for determining nearest full node from a light node in blockchain iot networks. International Journal of Computing and Digital Systems, 16(1):1–10, 2024.

[18] Mohammad Aliyan, Muhammad Zulkifl Hasan, Hammad Qayoom, Muhammad Zunnurain Hussain, Summaira Nosheen, Muzzamil Mustafa, Saad Hussain Chuhan, Muhammad Atif Yaqub, Rimsha Awan, and Afshan Bilal. Analysis and performance evaluation of various shortest path algorithms. In 2024 3rd International Conference for Innovation in Technology (INOCON), pages 1–16. IEEE,2024.

[19] Iza Shafinaz Mohamad Hashim and Akram Al-Hourani. Satellite visibility window estimation using doppler measurement for iot applications. IEEE Communications Letters, 27(3):956–960, 2023.

[20] Dhiraj Bhattacharjee, Pablo G. Madoery, Aizaz U. Chaudhry, Halim Yanikomeroglu, G¨une, s Karabulut Kurt, Peng Hu, Khaled Ahmed, and St´ephane Martel. On-demand routing in leo mega-constellations with dynamic laser intersatellite links. IEEE Transactions on Aerospace and Electronic Systems, pages 1–17, 2024.

[21] Bastian Knieling, Karsten Schindler, Amanda A Sickafoose, Michael J Person, Stephen E Levine, and Alfred Krabbe. Stellar occultations in the era of data mining and modern regression models: Using gaussian processes to analyze light curves and improve predictions. The Planetary Science Journal, 5(4):104, 2024.

[22] Krzysztof Socha and Marco Dorigo. Ant colony optimization for continuous domains. European journal of operational research, 185(3):1155–1173, 2008.

[23] Pavel Novoa-Hern´andez, Carlos Cruz Corona, and David A Pelta. Efficient multiswarm pso algorithms for dynamic environments. Memetic Computing, 3:163–174, 2011.

[24] Rahul Priyadarshi. Energy-efficient routing in wireless sensor networks: A metaheuristic and artificial intelligence-based approach: A comprehensive review. Archives of Computational Methods in Engineering, pages 1–29, 2024.

[25] Benjamin Danso Kwakye, Yongjun Li, Halima Habuba Mohamed, Evans Baidoo, and Theophilus Quachie Asenso. Particle guided metaheuristic algorithm for global optimization and feature selection problems. Expert Systems with Applications, 248:123362, 2024.

[26] Lucy Sumi and Shouvik Dey. Improved bounding box regression loss for weapon detection systems using deep learning. International Journal of Information Technology, pages 1–17, 2024.